Journal of Molecular Spectroscopy 348 (2018) 2–12

Contents lists available at ScienceDirect

Journal of Molecular Spectroscopy

journal homepage: www.elsevier.com/locate/jms

Measurement and computations of line shape parameters for the 12201 ← 03301, 11101 ← 10002 and 12201 ← 11102 self-broadened CO_2 Q-branches

Abdullah Al Mashwood [a], Adriana Predoi-Cross [a,*], V. Malathy Devi [b], Hoimonti Rozario [a], Brant Billinghurst [c]

[a] Department of Physics and Astronomy, University of Lethbridge, 4401 University Drive, Lethbridge, AB T1K 3M4, Canada
[b] Department of Physics, The College of William and Mary, Williamsburg, VA 23187, USA
[c] Far-Infrared Beamline, Canadian Light Source Inc., Saskatoon, SK S7N 2V3, Canada

ARTICLE INFO

Article history:
Received 27 October 2016
In revised form 7 February 2017
Accepted 18 August 2017
Available online 23 August 2017

ABSTRACT

Pure CO_2 spectra recorded at room temperature and different pressures (0.2–140 Torr) have been analyzed with the help of a fitting routine that takes into account asymmetries arising in the spectral lines due to pressure induced effects such as line mixing. The fitting procedure used in this study allows one to adjust the ro-vibrational constants for the band rather than fitting for individual line parameters. These constrained parameters greatly reduce the measurement uncertainties and allow us to observe the behavior of the weak lines corresponding to high *J* quantum numbers. We have also calculated line mixing parameters using approximations based on exponential nature of the energy difference between ground and upper vibrational states involved in the ro-vibrational band transitions. The calculated results show good agreement when compared with the experimentally determined parameters.

© 2017 Elsevier Inc. All rights reserved.

1. Introduction

The advent of fossil fuel from the pre-industrial period has resulted in a gradual increase of CO_2 concentration in the atmosphere (more than 30% increase) and has been one of the most important contributing factors to global warming [1]. In the Kyoto protocol, all countries from the United Nations had agreed upon the necessity for monitoring industrial CO_2 emission around the globe. Satellite based remote sensing devices such as the OCO-2 and GOSAT have been set to monitor the CO_2 concentration in air to help identify its impact and take necessary initiatives accordingly. Also, CO_2 can be found in the atmosphere of many other planets. For example, Mars has 95.3% CO_2 in its atmosphere. Therefore, CO_2 is considered to be of great interest to the spectroscopic community that focuses on atmospheric research of different planets. Studying the atmospheric evolution of once habitable planets like Mars is crucial for the future survival of life on Earth. CO_2 is considered to be a key element in making an atmosphere habitable for any kind of life form [2].

In order to accurately analyze the remotely retrieved spectroscopic data from terrestrial or planetary atmospheres, we need precise measurements of the various spectral line parameters for several molecular bands present in different planetary atmospheres. These parameters include line positions, intensities, pressure broadening and pressure-induced shift coefficients, and line mixing parameters. Our study focused on the three relatively weak bands of CO_2 located in the 15 μm spectral regions. These three bands can be considered to be ideal candidates for precise measurement of temperature in the atmosphere. In order to monitor the concentration of other gases in the air, one needs to know the temperature profiles accurately. Therefore, a careful approach has been followed to accurately characterize, analyze and retrieve the line shape parameters of pure CO_2 gas for the three bands: 12201 ← 03301 (centered about 757.5 cm^{-1} and shown in panel (A) of Fig. 1), 11101 ← 10002 (centered about 791.5 cm^{-1} and shown in panel (B) of Fig. 1), and 12201 ← 11102 (centered about 828.2 cm^{-1} and shown in panel (C) of Fig. 1), in their respective Q branches. In this study, a Bruker IFS-125HR Fourier transform spectrometer and, a multipass gas absorption cell able to keep the temperature constant during the experiments have been utilized to record all the spectra at room temperature in the appropriate spectral region covering the three CO_2 bands. A 99.95% pure natural sample of CO_2 was used to record the spectra.

2. Literature review

Several previous studies have discussed line parameters extracted from Q-branch transitions belonging to CO_2 absorption bands. L L. Strow and B.M. Gentry have reported the calculation

* Corresponding author.
E-mail address: adriana.predoicross@gmail.com (A. Predoi-Cross).

http://dx.doi.org/10.1016/j.jms.2017.08.009
0022-2852/© 2017 Elsevier Inc. All rights reserved.

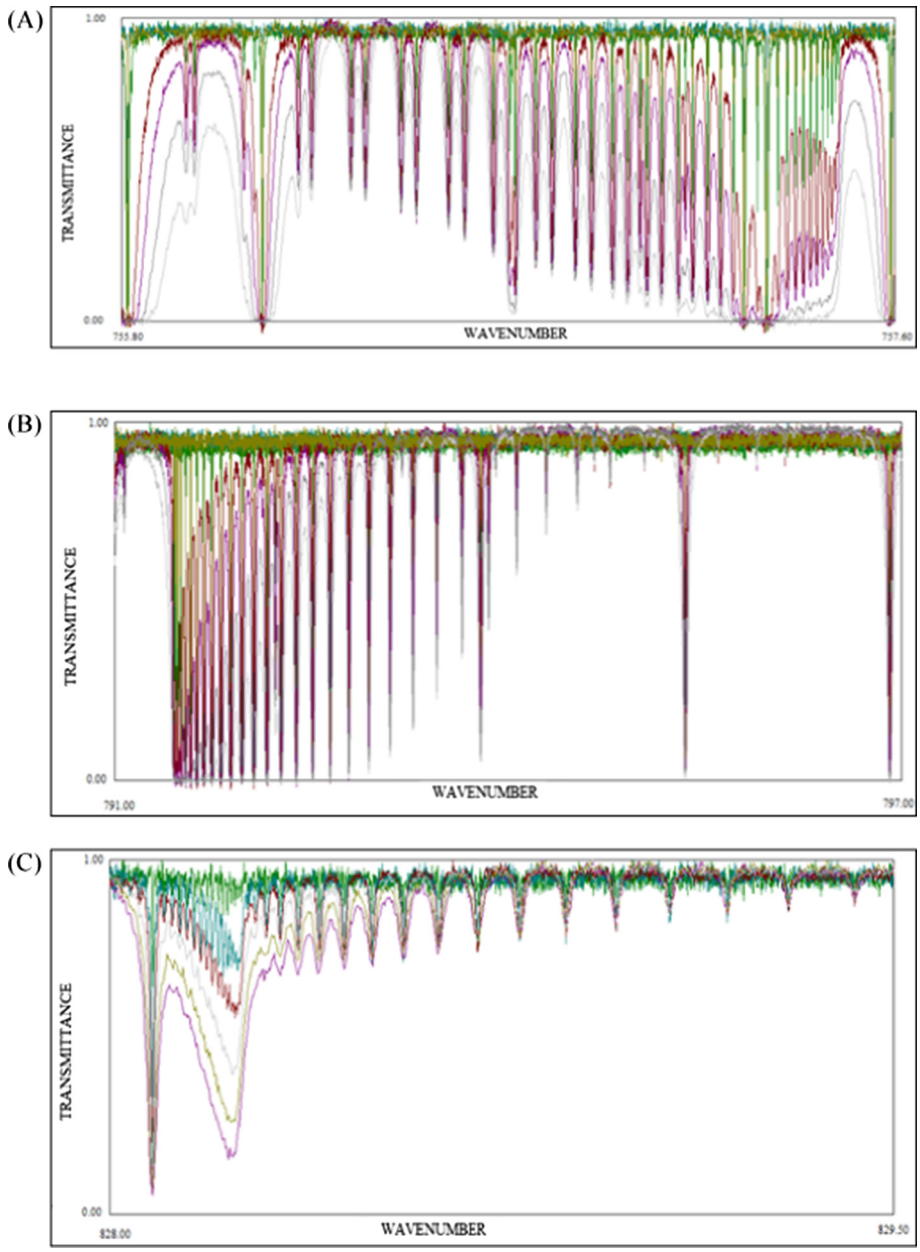

Fig. 1. Overlaid measured spectra of the three Q-branches of CO_2 plotted as a function of wavenumber (cm^{-1}). (A) 12201 ← 03301 band centered about 757.5 cm^{-1}, (B) 11101 ← 10002 band centered about 791.5 cm^{-1}, and (C) 12201 ← 11102 band centered about 828.2 cm^{-1}. The gas sample pressures range between 0.26 Torr and 140 Torr. All spectra were recorded at room-temperature (see Table 2 for details).

of line mixing parameters using a fitting law model for Q-branch lines in the band located at 1932.47 cm^{-1}. They recorded their spectra with a Tunable diode laser spectrometer (TDLS) instrument at gas sample pressures from 100 to 745 Torr and calculated line mixing coefficients for up to $J = 50$ using the relaxation matrix formalism. The calculated results agreed with the experiments within a few percent. A similar study was conducted by the same group for CO_2 broadened by N_2 for the Q-branch located at 2076 cm^{-1} [4]. The absorption coefficients measured from their experiment were 65% lower compared to the values computed using the Lorentzian line shape [4]. Line mixing coefficients were calculated and used to reproduce the absorption coefficients which agreed very well with the measured ones.

Another study was carried out by M. V. Tonkov et al. for both pure CO_2, CO_2-He and CO_2-Ar in the 580–850 cm^{-1} range [5]. The spectra were recorded at pressures ranging from a few Torr to 50 Torr. It was found that at higher sample pressures, the shapes of the Q-branch lines change significantly which deviates from Lorentzian approximation, which was considered to be due to line mixing.

Predoi-Cross et al. reported results from the spectroscopic analyses of pure CO_2 for the Q-branch transitions in the three bands $12^20 \leftarrow 01^10$, $20^00 \leftarrow 01^10$ and $11^10 \leftarrow 00^00$ [6]. A scaling law based on energy corrected sudden approximation was implemented to take into account weak line mixing effects and to predict transformation of line shape in these three bands at higher pressures. They also described Exponential Power Gap (EPG) law which is also used in the present study.

In this study we report line parameters obtained from analyzing pure CO_2 spectra in the 700–900 cm^{-1} range. A nonlinear least squares curve fitting algorithm capable of fitting multiple spectra (Labfit) simultaneously has been used. The software fits all the

spectra recorded at different pressures and retrieves spectral line parameters such as position and intensity along with pressure-broadened line shape parameters (broadening and shift coefficients). We were able to directly measure the line mixing coefficients for the series $12201 \leftarrow 03301$ and $11101 \leftarrow 10002$. In addition, we have calculated the line mixing parameters for these three bands using the Exponential Power Gap scaling law. The calculated and experimentally measured values have been reported in this paper in order to demonstrate the suitability of such calculations for similar future studies.

3. Experimental details

Measurements of highly accurate line parameters require high resolution, high signal to noise ratio spectra as well as comparatively small instrumental line shape. The Bruker IFS 125HR spectrometer located at the far-infrared beamline at the Canadian Light Source (CLS) has been used for our measurements. A total of 9 spectra of 99.95% pure CO_2 were recorded using the Globar source, all at room temperature and pressures ranging from 0.2 Torr to 140 Torr. A temperature-controlled multi-pass gas cell set for an optical path of 72.15 m was used in all measurements. The details of the setup are given in Table 1 while the summary of the experimental conditions of the CO_2 spectra analyzed in this study are listed in Table 2.

The spectra were calibrated to an accuracy better than 10^{-4} using the water vapor line positions taken from the HITRAN database [7]. These water lines appeared in the spectra due to residual water in the evacuated FTS chamber.

4. Spectroscopic analysis

In spectroscopic applications, accurate measurement of line shape parameters corresponding to molecular absorption of infrared radiation is of great importance. For example, different algorithms based on nonlinear least squares fitting principles have been developed by various research groups around the globe for spectral data analysis. The multispectrum nonlinear least squares fitting routine, developed by Benner et al. [8,9] is based upon Levenberg-Marquardt algorithm [10,11]. It minimizes the sum of the squares of the observed minus calculated residuals by fitting the spectral lines to a set of line shape parameters. The user has the freedom of fixing or adjusting (fitting) the various line parameters, such as spectral line positions, intensities, pressure-broadened half-width coefficients, their temperature dependence exponents, according to the specific application chosen.

Labfit is a weighted multispectrum fitting program. In most cases, for low to moderate pressure (<50 Torr but dependent upon the specific gas sample) regime, a Voigt line shape model which takes into account basic line parameters such as position, intensity, width and pressure shift is generally adequate for providing a good fit. As the sample pressure increases, adjacent lines tend to overlap, and the Voigt line shape model can no longer predict the transformation of line shapes within the experimental uncertainty limit, since the degree of correlation between pairs of various fitted parameters become more significant in such cases. One method of solving this problem is to carry out a constrained fitting of the spectra and to take into account the line mixing effects [12]. The method of constraint analysis is described in more details in the next section.

Previous studies have suggested, line mixing effects significantly change the line shapes for the Q-branch transitions in the bands located in the 700–850 cm^{-1} region [3]. In order to take into account asymmetries caused by collisional effects in the line shapes, the nonlinear least squares fitting routine utilizes off-diagonal relaxation matrix formalism. As noticed during our analysis, the absorption lines tend to overlap at higher pressures thus inducing line mixing among the various transitions. As previously stated, for example in Ref. [13], when the widths of the adjacent lines become comparable to the energy difference between individual transitions in a band, line mixing causes a transfer of intensity from the weaker to the stronger neighboring lines.

The degree of line mixing between two adjacent lines j and k can be represented by the off-diagonal elements of a complex relaxation matrix, whose diagonal elements are the pressure broadening (real part) and pressure-shift coefficients (imaginary part). The off-diagonal elements below and above the diagonal are related using the detailed balance equation, as described for instance in Ref. [9]. A summary of the relaxation matrix formalism is described in details in Section 6 of this paper. Fitting the spectra by taking into account line mixing significantly reduces the residual of the fit, as shown in Fig. 2.

A set of constraints were added to the fitting software in order to solve for the ro-vibrational (B, D, H) as well as for the transition moment constants (vibrational band strength S_v, and the Herman-Wallis-type coefficients a) corresponding to each band [12]. The general equations used for this constraint analysis are as follows:

$$\nu_i = G' - G'' + (B'J'[J'+1] - D'\{J'[J'+1]\}^2 + H'\{J'[J'+1]\}^3) - (B''J''[J''+1] - D''\{J''[J''+1]\}^2 + H''\{J''[J''+1]\}^3) \quad (1)$$

The expression used for band intensity parameters is given as,

$$S_i = \frac{S_v \nu_i L_i F}{Q_r \nu_0} \exp\left(\frac{-C_2 E''}{T_0}\right)\left[1 - \exp\left(\frac{-C_2 \nu_i}{T_0}\right)\right] \quad (2)$$

where

$$F = (1 + aJ(J+1))^2 \quad (3)$$

Table 1
Experimental setup used in the present study.

Configuration of the FTS used at the CLS	
Beam splitter and band pass	Ge/KBr (400–4800 cm^{-1})
Detector type and band pass	Ge:Cu (300–1850 cm^{-1})
Detector filter range	490–1190 cm^{-1}
Source aperture diameter	1.5 mm
Window material and band pass	KBr (400–5000 cm^{-1})
Carriage velocity	40 kHz
Spectral range	490–1190 cm^{-1}
Resolution	0.002 cm^{-1}
Gas sample	CO_2 99.95% purity from Praxair

Table 2
Experimental details of the nine spectra recorded using high-purity (99.95%) CO_2. All spectra were obtained in the 490–1190 cm^{-1} region at the Canadian Light Source facility and an absorption path of 72.15 m. The pressure measurements were accurate to ±0.05%. The *T*-type thermocouple used for measuring the temperature had an accuracy of ±1 °C for a temperature range of −200 to 400 °C.

No	Gas sample pressure (Torr)	Gas sample temperature (°C)
1	0.501	23.4
2	0.2564	23.4
3	1.99	23.7
4	16.344	23.6
5	94.80	23.7
6	75.744	23.6
7	50.437	23.5
8	140.00	23.9
9	20.99	23.6

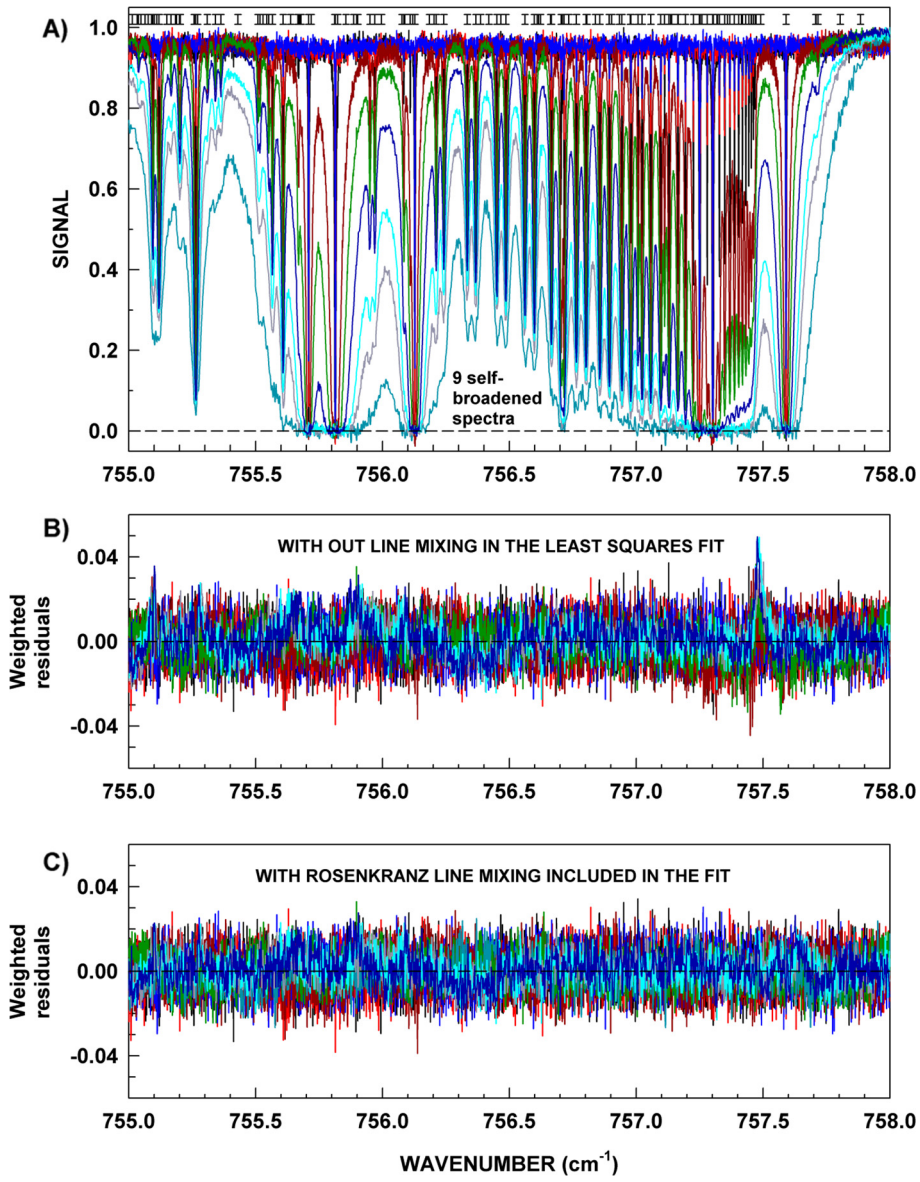

Fig. 2. A multispectrum non-linear least square fit of nine pure CO_2 spectra in the 12201 ← 03301 ($v_0 \sim 757.5\ cm^{-1}$) band. Including line mixing in the fit reduces the observed minus calculated residuals mainly near the band head as seen by comparing panels (B) and (C) of the figure. The short vertical lines at the top of panel (A) correspond to positions of lines included in the least squares fit.

Here, v_i corresponds to the line positions of the individual transitions whereas the upper and lower vibrational states are denoted by prime and double prime, respectively. In Eq. (2), L_i and C_2 are the Hönl-London factors and the second radiation constant. v_0 is the band center and Q_r corresponds to the rotational partition function. Q-branches are represented by the index m where m = J''. We have used a Voigt line shape model with line mixing to fit the CO_2 spectra. This methodology efficiently reduces the correlations between different fitted parameters.

The ro-vibrational constants belonging to the three bands (12201 ← 03301), (11101 ← 10002) and (12201 ← 11102) and the retrieved constants are listed in Tables 3a–3c. The fixed constants for the lower vibrational levels were taken from Table 3 of Ref. [14] which also lists the ro-vibrational constants corresponding to the upper vibrational levels. The measured values from our constrained multispectrum analysis show good agreement with the theoretically computed constants listed in Ref. [14].

Fig. 2 shows the multispectrum least square fit of nine self-broadened spectra of pure CO_2 in the 12201 ← 03301 band located near 757.48 cm^{-1} region. Here, the weighted fit residuals are shown in the lower two graphs with and without line mixing taken into account. We implemented the measured Rosenkranz (weak) line mixing for the 12201 ← 03301 (see Fig. 2) and the 11101 ← 10002 bands of CO_2, and the calculated ones for the third band. The improvements seen in the fit residuals with line mixing included in the least squares fits are clearly seen in panel (c) of Fig. 2.

Applying the fitting procedure described in [8], the Lorentzian half width and the shifted positions of the individual absorption lines were found by implementing the following equations [12] applicable to room temperature measurements.

$$\gamma(p,T) = p \times \left[\gamma^0_{self}(p_0,T_0) \times \left[\frac{T_0}{T}\right]^n\right], \tag{4}$$

Table 3a
Ro-vibrational and band intensity parameters (cm^{-1}/molecule. cm^{-2}) at 296 K of the 12201 ← 03301 band in CO_2. The fixed constants are taken from Table 3 of Ref. [14] and are presented here with as many significant figures as the corresponding fitted values. The fit errors are one standard deviation.

12201 ← 03301 Band (Ro-vibrational Constants)		12201 ← 03301 Band (Intensity parameters)	
Parameter (cm^{-1})	Value	Parameter	Value
$G' - G''$	757.47896503 ± 0.00000787	S_v (cm^{-1}/(molecule cm^{-2}))	$(0.6274 \pm 0.0017) \times 10^{-22}$
B_e'	0.391562768 ± 0.000000048	a	$(3.5538 \pm 0.8989) \times 10^{-6}$
D_e'	$(1.41897 \pm 0.00064) \times 10^{-7}$		
H_e'	$(-0.6133 \pm 0.0202) \times 10^{-12}$		
B_f'	0.391566903 ± 0.000000046		
D_f'	$(1.28717 \pm 0.00058) \times 10^{-7}$		
H_f'	$(0.2065 \pm 0.0172) \times 10^{-12}$		
B_e''(Fixed)	0.392398537		
D_e''(Fixed)	0.140969×10^{-6}		
H_e''(Fixed)	0		
B_f''(Fixed)	0.392394358		
D_f''(Fixed)	0.140893×10^{-6}		
H_f''(Fixed)	0		

Table 3b
Ro-vibrational and band intensity parameters (cm^{-1}/molecule. cm^{-2}) at 296 K of the 11101 ← 10002 band. The fixed constants are taken from Table 3 of Ref. [14] and are presented here with as many significant figures as the corresponding fitted values. The fit errors are one standard deviation.

11101 ← 10002 Band (Rotational Constants)		11101 ← 10002 Band (Intensity parameters)	
Parameter (cm^{-1})	Value	Parameter	Value
$G' - G''$	791.4475845 ± 0.00000411	S_v (cm^{-1}/(molecule cm^{-2}))	$(3.687 \pm 0.012) \times 10^{-22}$
B_e'(Fixed)	0.39040968	a	$(-0.30998 \pm 0.01078) \times 10^{-4}$
D_e'(Fixed)	1.25861×10^{-7}		
H_e'(Fixed)	9.31792×10^{-14}		
B_f'	0.391334071 ± 0.000000017		
D_f'	$(0.121250 \pm 0.000017) \times 10^{-6}$		
H_f'	$(0.7354 \pm 0.0451) \times 10^{-13}$		
B''(Fixed)	0.390482283		
D''(Fixed)	0.157203×10^{-6}		
H''(Fixed)	2.41827×10^{-13}		

Table 3c
Ro-vibrational and band intensity parameters (cm^{-1}/molecule. cm^{-2}) at 296 K of the 12201 ← 11102 band. The fixed constants are taken from Table 3 of Ref. [14] and are presented here with as many significant figures as the corresponding fitted values. The fit errors are one standard deviation.

12201 ← 11102 Band (Rotational Constants)		12201 ← 11102 Band (Intensity parameters)	
Parameter (cm^{-1})	Value	Parameter	Value
$G' - G''$	828.2546246 ± 0.0000435	S_v (cm^{-1}/(molecule cm^{-2}))	$(0.484 \pm 0.004) \times 10^{-23}$
B_e'	0.39154902 ± 0.00000015	a	$(-4.6939 \pm 0.9330) \times 10^{-5}$
D_e'	$(1.44689 \pm 0.00104) \times 10^{-7}$		
H_e'(Fixed)	7.13899×10^{-13}		
B_f'	0.39154766 ± 0.00000017		
D_f'	$(1.28249 \pm 0.00128) \times 10^{-7}$		
H_f'(Fixed)	0.90038×10^{-13}		
B_e''(Fixed)	0.390745013		
D_e''(Fixed)	0.149498×10^{-6}		
H_e''(Fixed)	0.1118×10^{-12}		
B_f''(Fixed)	0.391690235		
D_f''(Fixed)	0.156290×10^{-6}		
H_f''(Fixed)	0.1008×10^{-12}		

$$\upsilon(p,T) = \upsilon_0 + p \times [\delta^0_{self}(T)], \quad (5)$$

γ^0 and δ^0 in Eqs. (4) and (5) are the pressure broadening and pressure-shift coefficients at $T_0 = 296$ K, in units of cm^{-1} atm^{-1}. $\gamma(p,T)$ and $\upsilon(p,T)$ are the Lorentz half-widths (in cm^{-1}) and line positions (in cm^{-1}) at pressure p and temperature T. n in Eq. (4) is the temperature dependence exponent corresponding to the pressure-broadening coefficient. In our case, we recorded all the spectra at room temperature and hence the value of n is 1 in our case.

The retrieved line positions, intensities and broadening coefficients for the three bands are reported in Tables 4a–4c. The uncertainties associated with each parameter were found using the method introduced by Whittaker and Robinson [15], implemented in Labfit. Benner et al. have briefly described this method in Ref. [8]. In the present analysis, since the transitions are close to each other, we did not adjust individual pressure-shift coefficients. Instead, we assumed the self-shift coefficients to be the same for all transitions in each Q branch (-0.003 cm^{-1} atm^{-1} and -0.002 cm^{-1} atm^{-1} for the 12201 ← 03301 and the 11101 ← 10002 band, respectively).

Comparisons between line positions from present study and the HITRAN [7] and GEISA [16] databases are shown in Fig. 3. To com-

Table 4a
Line parameters retrieved at 296 K for the Q branch lines in the 12201 ← 03301 band of CO_2. The fit uncertainties are one standard deviation.

Line label	m	Line positions (cm^{-1})	Line intensities (cm^{-1}/(cm^{-2}/molecule))	Self-broadening coefficient (cm^{-1} atm^{-1}) at 296 K
Q 3e	3	757.4690(8)	$8.14(2) \times 10^{-25}$	0.1351(5)
Q 4f	4	757.4623(7)	$1.44(4) \times 10^{-24}$	0.1347(4)
Q 5e	5	757.4540(7)	$1.98(5) \times 10^{-24}$	0.1305(3)
Q 6f	6	757.4440(7)	$2.45(6) \times 10^{-24}$	0.1238(3)
Q 7e	7	757.4324(6)	$2.87(7) \times 10^{-24}$	0.1218(2)
Q 8f	8	757.4191(6)	$3.24(8) \times 10^{-24}$	0.1203(2)
Q 9e	9	757.4042(6)	$3.56(9) \times 10^{-24}$	0.1217(2)
Q 10f	10	757.3875(6)	$3.84(9) \times 10^{-24}$	0.1167(2)
Q 11e	11	757.3694(5)	$4.07(10) \times 10^{-24}$	0.1183(2)
Q 12f	12	757.3492(6)	$4.26(10) \times 10^{-24}$	0.1157(3)
Q 13e	13	757.3280(5)	$4.40(10) \times 10^{-24}$	0.1149(4)
Q 14f	14	757.3043(6)	$4.51(10) \times 10^{-24}$	0.0972(27)
Q 15e	15	757.2801(6)	$4.57(10) \times 10^{-24}$	0.1234(5)
Q 16f	16	757.2527(6)	$4.59(9) \times 10^{-24}$	0.0984(10)
Q 17e	17	757.2256(6)	$4.58(9) \times 10^{-24}$	0.1083(3)
Q 18f	18	757.1944(7)	$4.53(9) \times 10^{-24}$	0.1059(2)
Q 19e	19	757.1647(7)	$4.45(8) \times 10^{-24}$	0.1045(2)
Q 20f	20	757.1295(8)	$4.34(8) \times 10^{-24}$	0.1070(2)
Q 21e	21	757.0974(7)	$4.21(8) \times 10^{-24}$	0.1025(2)
Q 22f	22	757.0578(8)	$4.06(7) \times 10^{-24}$	0.1065(2)
Q 23e	23	757.0237(8)	$3.89(7) \times 10^{-24}$	0.1038(2)
Q 24f	24	756.9795(8)	$3.71(7) \times 10^{-24}$	0.0982(2)
Q 25e	25	756.9436(8)	$3.51(6) \times 10^{-24}$	0.0979(2)
Q 26f	26	756.8945(8)	$3.31(6) \times 10^{-24}$	0.0988(2)
Q 27e	27	756.8573(8)	$3.11(6) \times 10^{-24}$	0.0986(2)
Q 28f	28	756.8027(8)	$2.90(6) \times 10^{-24}$	0.1015(2)
Q 29e	29	756.7649(9)	$2.69(6) \times 10^{-24}$	0.0936(2)
Q 30f	30	756.7042(9)	$2.48(6) \times 10^{-24}$	0.0984(2)
Q 31e	31	756.6662(10)	$2.28(6) \times 10^{-24}$	0.0969(2)
Q 32f	32	756.5990(11)	$2.09(5) \times 10^{-24}$	0.0922(2)
Q 33e	33	756.5616(12)	$1.90(5) \times 10^{-24}$	0.0917(2)
Q 34f	34	756.4869(13)	$1.72(5) \times 10^{-24}$	0.0882(2)
Q 35e	35	756.4510(14)	$1.55(5) \times 10^{-24}$	0.0869(2)
Q 36f	36	756.3681(16)	$1.39(5) \times 10^{-24}$	0.0882(2)
Q 37e	37	756.3345(17)	$1.24(5) \times 10^{-24}$	0.0835(2)
Q 38f	38	756.2423(18)	$1.11(4) \times 10^{-24}$	0.0826(2)
Q 39e	39	756.2122(20)	$9.78(4) \times 10^{-25}$	0.0835(2)
Q 40f	40	756.1098(21)	$8.62(4) \times 10^{-25}$	0.0896(4)
Q 41e	41	756.0843(23)	$7.57(4) \times 10^{-25}$	0.0797(3)
Q 42f	42	755.9702(23)	$6.61(3) \times 10^{-25}$	0.0762(2)
Q 43e	43	755.9508(26)	$5.75(3) \times 10^{-25}$	0.0864(3)

pare the precision achieved in our retrieved line positions, we have illustrated the residuals of line positions from our experimental values and the two databases [7,16]. Six sets of results for the three CO_2 bands are plotted in Fig. 3. It is clear that the 11101 ← 10002 band transitions are in very good agreement with HITRAN values for J up to 45. The line positions for the 12201 ← 03301 band transitions are in good agreement for only up to $J = 27$. The 12201 ← 11102 band is the weakest among the three bands of interest. As expected, the observed line positions in this band show the least agreement with HITRAN values and the residuals deviate randomly as shown in Fig. 3. In the case of comparisons with GEISA database, the second band (11101 ← 10002) shows the best agreement with the observation whereas the position difference plotted for two bands are consistently high even for lower J lines, which could due to a difference in calibration standards for the source data entered in the databases.

In order to verify the intensities of the corresponding lines listed in Tables 4a–4c, we have determined the ratio of intensities between our measured values and the HITRAN and the GEISA databases. As can be seen in Fig. 4 the best agreement between observed and Ref. [7,16] were found for the 11101 ← 10002 band, while the agreement is least for the 12201 ← 11102 band transitions. Measured intensity values and the HITRAN values are in better agreement compared to values with the GEISA database. The line position and intensity values found in HITRAN and GEISA databases differ slightly from each other, which results in a difference in agreement when making comparisons with experimentally measured values as can be seen in Figs. 3 and 4.

5. Exponential Power Gap (EPG) calculations for line mixing coefficients

We followed the approach adopted by Levy et al. [17] whereby the bands of CO_2 are taken into account as a whole. Two sets of approximations were implemented in our calculations: (1) the binary collisions and impact approximations and, (2) the factorized density matrix formalism [17,18]. Levy et al. [17] considered a relaxation matrix that exhibits as an entire band of CO_2 with all the physical parameters associated with it. As mentioned earlier, the diagonal elements of this matrix are the Lorentz broadening (real part) and the line shift coefficients (imaginary part). The off-diagonal elements determine the line mixing coefficients. The EPG law enables us to calculate the elements of the relaxation matrix (see Table 5).

Based on the EPG approximation collisional transfer rates of the molecule of interest in going from ground state (k) to a higher (j) state can be expressed as,

$$\kappa_{jk} = a\left[\frac{|\Delta E_{jk}|}{B_0}\right]^{-b} \exp\left(\frac{-c|\Delta E_{jk}|}{k_B T}\right) \quad (6)$$

Table 4b
Line parameters retrieved at 296 K for the Q branch lines of the 11101 ← 10002 band. The fit uncertainties are one standard deviation.

Line label	m	Line positions (cm^{-1})	Line intensities (cm^{-1}/(cm^{-2}/molecule))	Self-broadening coefficient (cm^{-1} atm^{-1})
Q 2e	2	791.4527(4)	$6.91(2) \times 10^{-24}$	0.1249(32)
Q 4e	4	791.4646(4)	$1.21(4) \times 10^{-23}$	0.1283(35)
Q 6e	6	791.4834(4)	$1.67(6) \times 10^{-23}$	0.1286(23)
Q 8e	8	791.5091(3)	$2.07(7) \times 10^{-23}$	0.1193(15)
Q10e	10	791.5417(3)	$2.37(8) \times 10^{-23}$	0.1113(12)
Q12e	12	791.5813(3)	$2.58(8) \times 10^{-23}$	0.1108(10)
Q14e	14	791.6280(2)	$2.69(8) \times 10^{-23}$	0.1097(9)
Q16e	16	791.6819(2)	$2.71(8) \times 10^{-23}$	0.1074(8)
Q18e	18	791.7431(2)	$2.65(8) \times 10^{-23}$	0.1058(8)
Q20e	20	791.8117(3)	$2.52(7) \times 10^{-23}$	0.1024(8)
Q22e	22	791.8878(3)	$2.34(6) \times 10^{-23}$	0.1029(8)
Q24e	24	791.9716(3)	$2.12(6) \times 10^{-23}$	0.1012(8)
Q26e	26	792.0632(3)	$1.87(5) \times 10^{-23}$	0.0967(7)
Q28e	28	792.1629(3)	$1.62(4) \times 10^{-23}$	0.0949(8)
Q30e	30	792.2707(3)	$1.38(3) \times 10^{-23}$	0.0927(8)
Q32e	32	792.3870(3)	$1.15(3) \times 10^{-23}$	0.0887(8)
Q34e	34	792.5118(3)	$9.38(2) \times 10^{-24}$	0.0894(9)
Q36e	36	792.6456(4)	$7.51(2) \times 10^{-24}$	0.0855(9)
Q38e	38	792.7884(4)	$5.91(2) \times 10^{-24}$	0.0871(11)
Q40e	40	792.9405(5)	$4.56(1) \times 10^{-24}$	0.0868(12)
Q42e	42	793.1022(5)	$3.46(1) \times 10^{-24}$	0.0809(12)
Q44e	44	793.2738(6)	$2.57(1) \times 10^{-24}$	0.0806(13)
Q46e	46	793.4555(7)	$1.88(1) \times 10^{-24}$	0.0735(13)
Q48e	48	793.6477(8)	$1.35(1) \times 10^{-24}$	0.0740(15)
Q50e	50	793.8506(10)	$9.55(0) \times 10^{-25}$	0.0759(18)
Q52e	52	794.0647(14)	$6.63(0) \times 10^{-25}$	0.0735(21)
Q54e	54	794.2901(20)	$4.53(0) \times 10^{-25}$	0.0734(28)

Table 4c
Line parameters retrieved at 296 K for the Q branch lines of the 12201 ← 11102 band of CO_2. The fit uncertainties are one standard deviation.

Line label	m	Line positions (cm^{-1})	Line intensities (cm^{-1}/(cm^{-2}/molecule))	Self-broadening coefficient (cm^{-1} atm^{-1})
Q 2f	2	828.2538(4)	$6.10(1) \times 10^{-26}$	0.0937(13)
Q 3e	3	828.2643(4)	$1.05(2) \times 10^{-25}$	0.1083(4)
Q 4f	4	828.2518(4)	$1.43(2) \times 10^{-25}$	0.1122(9)
Q 5e	5	828.2787(3)	$1.78(3) \times 10^{-25}$	0.1098(2)
Q 6f	6	828.2487(3)	$2.10(3) \times 10^{-25}$	0.0963(4)
Q 7e	7	828.2996(3)	$2.38(3) \times 10^{-25}$	0.1152(2)
Q 8f	8	828.2445(2)	$2.64(4) \times 10^{-25}$	0.0906(2)
Q 9e	9	828.3207(2)	$2.86(4) \times 10^{-25}$	0.1133(1)
Q10f	10	828.2392(2)	$3.05(4) \times 10^{-25}$	0.0907(2)
Q11e	11	828.3609(3)	$3.21(4) \times 10^{-25}$	0.1122(1)
Q12f	12	828.2329(3)	$3.33(4) \times 10^{-25}$	0.0874(1)
Q13e	13	828.4014(3)	$3.42(4) \times 10^{-25}$	0.1106(1)
Q14f	14	828.2255(3)	$3.48(4) \times 10^{-25}$	0.0844(1)
Q15e	15	828.4485(3)	$3.51(4) \times 10^{-25}$	0.1061(1)
Q16f	16	828.2171(3)	$3.50(4) \times 10^{-25}$	0.0828(1)
Q17e	17	828.5022(3)	$3.48(4) \times 10^{-25}$	0.1078(1)
Q18f	18	828.2077(3)	$3.42(3) \times 10^{-25}$	0.0831(1)
Q19e	19	828.5627(4)	$3.35(4) \times 10^{-25}$	0.1057(1)
Q20f	20	828.1974(4)	$3.24(4) \times 10^{-25}$	0.0820(1)
Q21e	21	828.6300(5)	$3.14(4) \times 10^{-25}$	0.1028(1)
Q22f	22	828.1862(5)	$3.00(4) \times 10^{-25}$	0.0815(1)
Q23e	23	828.7042(6)	$2.87(4) \times 10^{-25}$	0.1028(1)
Q24f	24	828.1742(7)	$2.71(4) \times 10^{-25}$	0.0806(1)
Q25e	25	828.7853(8)	$2.56(4) \times 10^{-25}$	0.0995(1)
Q26f	26	828.1614(10)	$2.39(4) \times 10^{-25}$	0.0828(1)
Q27e	27	828.8736(14)	$2.24(5) \times 10^{-25}$	0.0979(1)
Q28f	28	828.1479(20)	$2.06(5) \times 10^{-25}$	0.0824(1)
Q29e	29	828.9690(29)	$1.91(5) \times 10^{-25}$	0.0956(1)
Q30f	30	828.1338(41)	$1.74(5) \times 10^{-25}$	0.0825(1)
Q31e	31	829.0717(57)	$1.60(5) \times 10^{-25}$	0.0913(1)
Q32f	32	828.1192(77)	$1.44(5) \times 10^{-25}$	0.0800(2)
Q33e	33	829.1819(103)	$1.31(4) \times 10^{-25}$	0.0900(1)
Q34f	34	828.1040(135)	$1.17(4) \times 10^{-25}$	0.0756(2)
Q35e	35	829.2996(174)	$1.06(4) \times 10^{-25}$	0.0833(2)

Here, ΔE_{jk} is the energy difference between j and k levels, B_0 is the rotational constant and a, b, c are dimensionless parameters. At a constant temperature and pressure the rate constant in Eq. (6) is related to the population of the levels j and k by the detailed balance equation:

$$\rho_k \kappa_{jk} = \rho_j \kappa_{kj} \quad (7)$$

where ρ_k and ρ_k are the population of level k and j respectively. The collisional transfer rate is related to the diagonal elements of the relaxation matrix using:

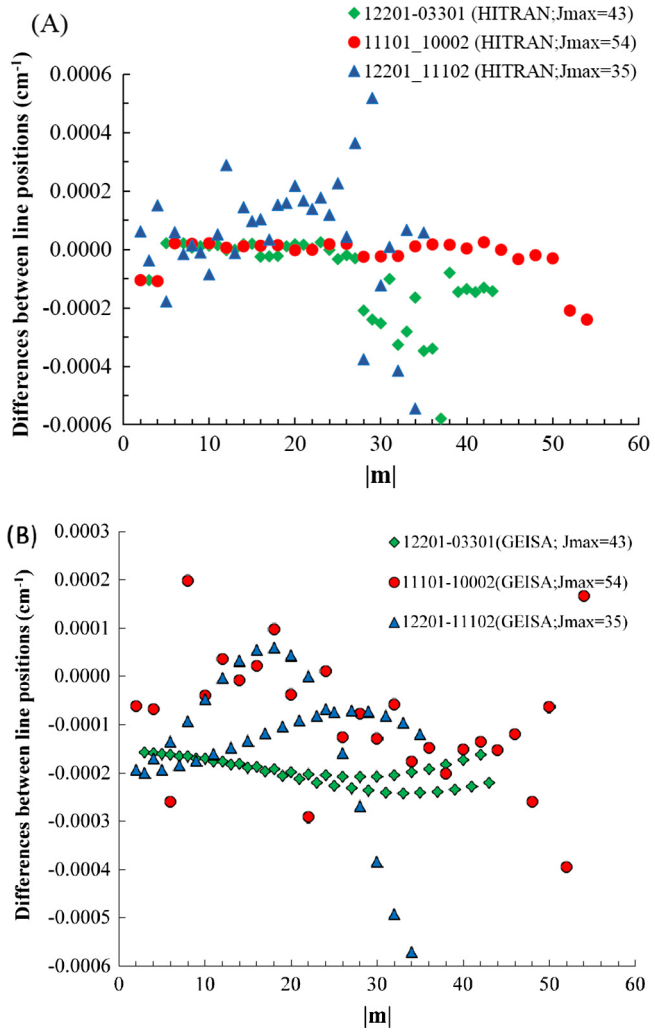

Fig. 3. Differences between line positions in each of the three CO2 bands analyzed in this work and the HITRAN [7] (panel (A)) and the GEISA [16] (panel (B)) databases. For database transitions the absolute uncertainty in cm^{-1} is larger than 0.0001 and less than 0.001.

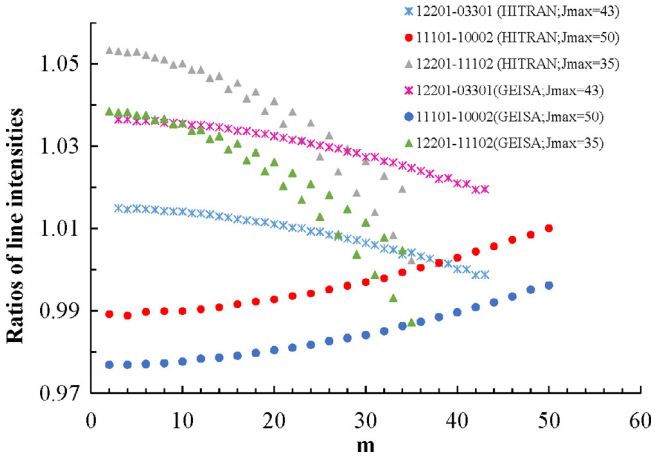

Fig. 4. Ratios of line intensities between present measurements and HITRAN [7] or GEISA [16] databases for each of the three CO2 bands analyzed in this study. The relative uncertainty in line intensities for database values is in the 20% range.

Table 5
The values of the adjustable parameters a, b and c from Eq. (6) in the present study for the three bands of CO_2. The fit errors are one standard deviation.

EPG parameters	12201 ← 03301	11101 ← 10002	12201 ← 11102
a	0.018(7)	0.053(1)	0.018(2)
b	0.333(1)	0.254(6)	0.328(4)
c	1.140(3)	1.340(7)	1.170(1)

$$W_{kk} = 1/2\left[\sum_j \kappa_{jk}\right]_{upper} + 1/2\left[\sum_j \kappa_{jk}\right]_{lower} \quad (8)$$

where upper and lower correspond to the upper and lower vibrational states respectively. The off-diagonal elements which correspond to the line mixing effects can be calculated from the following expression:

$$W_{jk} = \beta\kappa_{jk} \quad (9)$$

The parameters a, b, c can be determined using a nonlinear least squares fit to the broadening coefficients with the sum rule for the off-diagonal elements being fulfilled. The sum rule ensured that the matrix elements of the same column add to zero. The value of β in our study was set to 0.56, this being the value that gives the best agreement between the measured and calculated line mixing coefficients. The line mixing coefficient can be found from the expression:

$$Y_{ok}(T) = 2\sum_{j\neq k}\frac{d_j}{d_k}\frac{W_{jk}}{\nu_k - \nu_j} \quad (10)$$

where d_j and d_k are the dipole matrix elements while ν_j and ν_k correspond to the line positions (cm^{-1}) of the corresponding transitions. As the calculated values in Table 6 suggests, the even and odd J values have slightly different trends for line mixing coefficients corresponding to 12201 ← 03301 band. The measured line mixing parameters have significantly scattered values to be able to relate to this distinguishing trend. The level of scatter in the measured values may be because the highest pressure in our spectra is 140 Torr which makes it difficult for the fitting routine to reproduce the observed spectra accurately. The disagreement between the observed and calculated line mixing values for 11101 ← 10002 band can be explained in a similar way.

6. Comparison between observed and calculated results

Comparisons between line positions from the present study and the HITRAN [7] and GEISA [16] databases are shown in Fig. 3. To compare the precision achieved in our retrieved line positions, we have illustrated the residuals of line positions from our experimental values and the two databases [7,16]. Six sets of results for the three CO_2 bands are plotted in Fig. 3. It is clear that the 11101 ← 10002 band transitions are in very good agreement with HITRAN values for J up to 45. The line positions for the 12201 ← 03301 band transitions are in good agreement up to $J = 27$. The 12201 ← 11102 band is the weakest among the three bands of interest. As expected, the observed line positions in this band show the least agreement with HITRAN values and the residuals deviate randomly as shown in Fig. 3(A).

In the case of comparisons with GEISA database shown in Fig. 3 (B), the second band (11101 ← 10002) shows the best agreement with the observation whereas the position difference plotted for the first and the third bands are consistently high even for lower J lines, which could indicate a difference in calibration standards between two databases.

In order to verify the intensities of the lines listed in Tables 4a–4c, we have determined the ratio of intensities between our measured values and the HITRAN and the GEISA databases. As can be seen in Fig. 4 the best agreement between observed and Ref. [7,16] were found for the 11101 ← 10002 band, while the agreement is least for the 12201 ← 11102 band transitions. Overall, the measured intensity values are in better agreement with the values stored in the HITRAN database, compared to values from the GEISA database. The line positions and intensity values found in HITRAN and GEISA databases differ slightly from each other, which results in a difference in agreement when making comparisons with experimentally measured values as shown in Figs. 3 and 4.

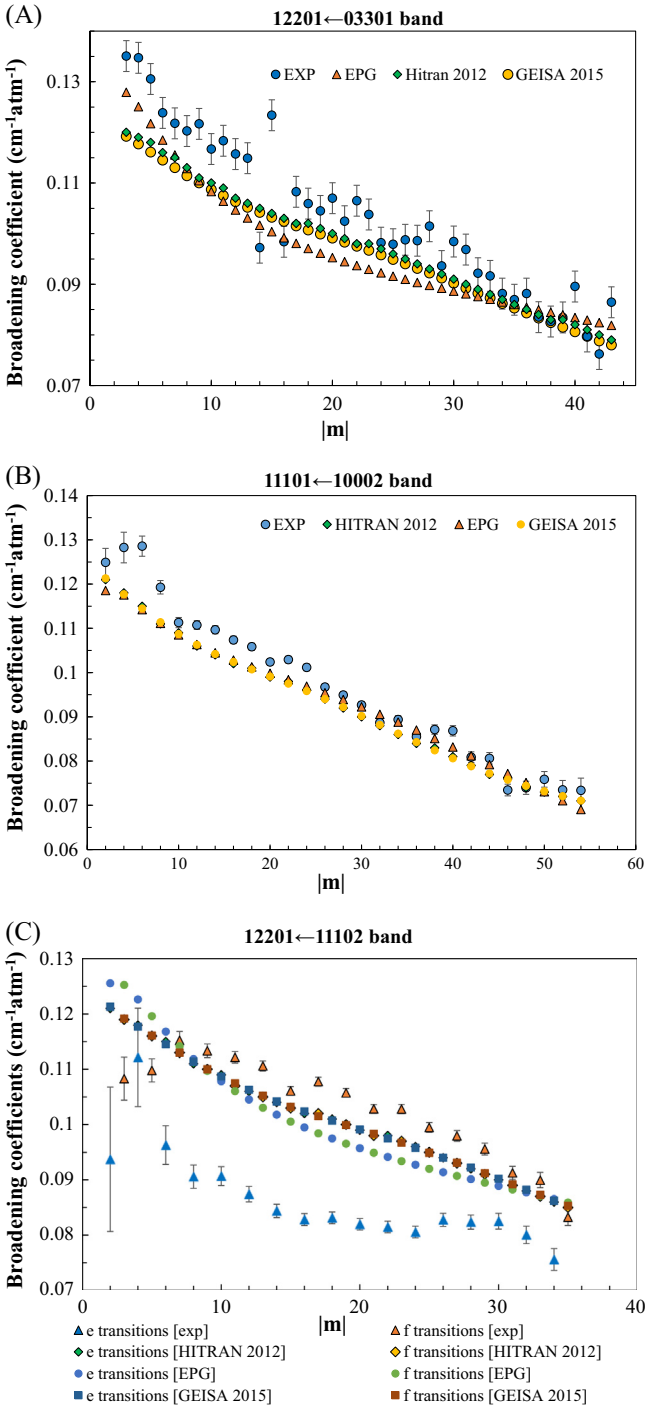

Fig. 5. Comparisons of self-broadened half-width coefficients between present measurements and the HITRAN [7] and GEISA [16] databases along with the calculated (EPG) values for the (A) 12201 ← 03301, (B) 11101 ← 10002 and (C) 12201 ← 11102 bands of CO2. Uncertainties associated with measured broadening coefficients are shown as error bars.

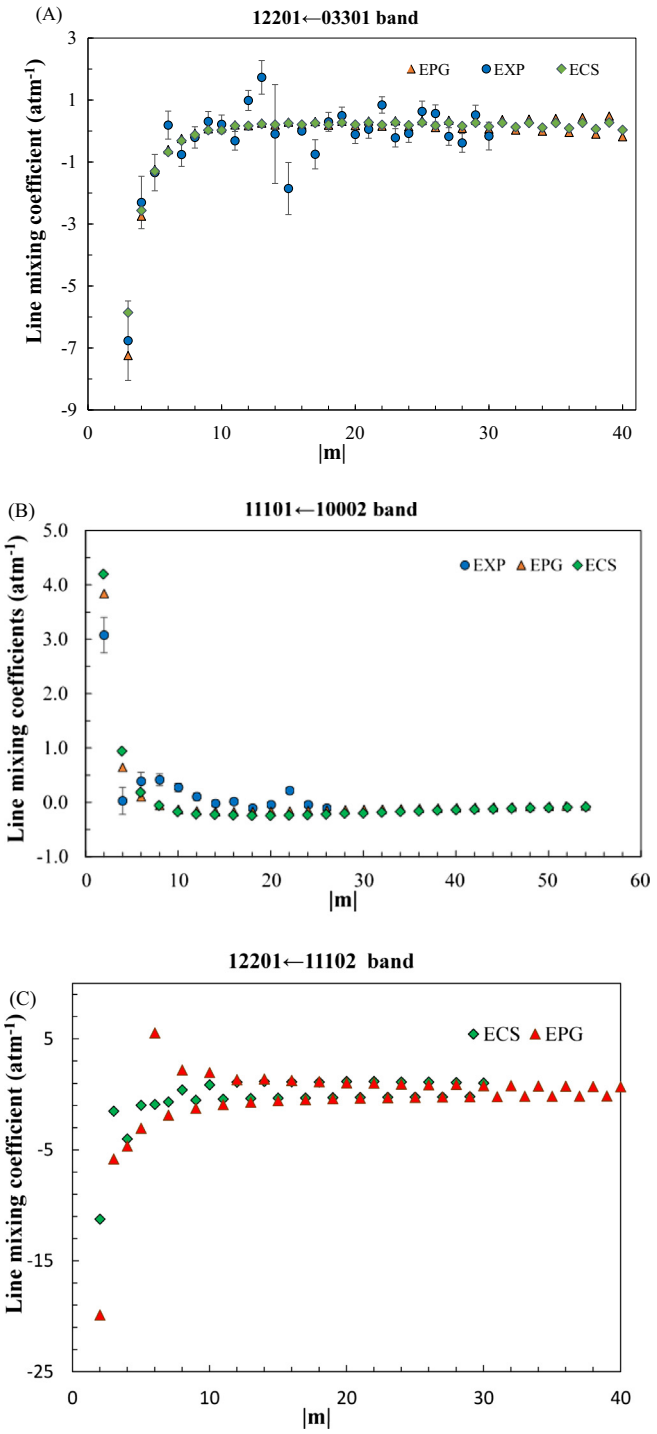

Fig. 6. (A) Comparison of self line mixing coefficients between observed and calculated (EPG & ECS) values for the 12201 ← 03301 band of CO_2. The experimentally measured values are shown with error bars representing uncertainties associated with non-linear fitting. (B) Comparison of self line mixing coefficients between observed and calculated (EPG & ECS) values from 11101 ← 10002 band. The experimentally measured values are shown with error bars representing uncertainties associated with non-linear fitting. (C) Calculated (EPG & ECS) self-line mixing coefficients from 12201 ← 11102 band. In all panels the ECS parameters were taken from the AER (Atmospheric and Environmental Research [http://rtweb.aer.com]) line parameter database.

The line positions and intensities listed in HITRAN [7] for the three CO_2 bands were calculated by Drs. S. Tashkun and V. Perevalov and provided as private communication. They used empirically obtained energy levels from effective Hamiltonian to calculate the line positions of 12201 ← 03301 band, whereas the line positions of the other two bands, 11101 ← 10002 and 12201 ← 11102 were calculated using the Ritz approach [21]. The line intensities were calculated using effective dipole moment function. The broadening coefficients corresponding to these three band transitions were calculated by Gamache and Lamouroux [20]. The line positions and intensities listed in GEISA database [16] for transitions in all three bands are calculated values obtained from the most recent version of CDSD-296 databank [21] whereas the broadening coefficients are measured values listed in a recent database [22].

Comparisons between measured and calculated values for broadening coefficients for the three CO_2 bands obtained using the EPG method, with corresponding values in the HITRAN and GIESA databases are shown in Fig. 5a–c. As the graphs suggest, all the four sets of values agree within 93.5% for 12201 ← 03301 band and 97.5% for 11101 ← 10002 band. For the 12201 ← 11102 band the agreement is about 88.6%. The measured broadening coefficients corresponding to the 12201 ← 03301 band show some scatter but an overall steady decreasing trend. The scatter may be due to the fact that the highest pressure in our spectra is 140 Torr as well as due to the correlation between broadening and line mixing parameters which becomes more significant at higher pressures. We did not constrain the broadening coefficients as we did for position and intensity which in turn induce greater uncertainty in their measured values.

The broadening coefficients from EPG calculation, HITRAN [7] and GIESA [16] databases show very smooth trends as shown in Fig. 5a. Fig. 5b shows broadening coefficients for the strongest of the three bands, 11101 ← 10002. As seen in the graphs, the measured values of this parameter show a similar smoothly descending trend as the calculated values as well as the values form the HITRAN and GIESA databases. In Fig. 5c the measured broadening coefficients belonging to e (even J) and f (odd J) type transitions from 12201 ← 11102 band show completely different trends suggesting two different types of pressure induced effects occurring for the same Q branch transitions. These results do not agree either with the calculated values from EPG approximation or the HITRAN and GIESA database values.

The measured and calculated values of line mixing coefficients for the 12201 ← 03301, 11101 ← 10002 and 12201 ← 11102 band are listed in Table 6. For the 12201-03301 band we could measure line mixing for up to $J = 30$ and for 11101 ← 10002 band up to $J = 26$. We were not able to extract line mixing parameters for 12201 ← 11102 band transitions because of the weakness of the band. The calculated values (EPG) for the line mixing coefficients for this band are listed in Table 6. For lines beyond the highest J listed in this table, the values for line mixing parameter are negligible and assumed to be zero in the solution.

In Fig. 6a and b we have compared our observations and calculated results (EPG) for line mixing coefficients for the first two

Table 6
Measured and calculated (EPG) line mixing coefficients (in atm^{-1}) for the three CO_2 bands. The fit errors are one standard deviation.

12201 ← 03301			11101 ← 10002			12201 ← 11102	
m	Observed (atm^{-1})	Calculated (atm^{-1})	m	Observed (atm^{-1})	Calculated (atm^{-1})	m	Calculated (atm^{-1})
3	−6.8(13)	−7.243	2	3.10(32)	3.839	2	−19.8742
4	−2.3(9)	−2.746	4	0.03(24)	0.642	3	−5.8265
5	−1.3(12)	−1.241	6	0.38(17)	0.101	4	−4.6581
6	0.2(1)	−0.600	8	0.41(11)	−0.060	5	−3.0481
7	−0.8(4)	−0.239	10	0.27(7)	−0.129	6	5.5395
8	−0.2(3)	−0.077	12	0.10(6)	−0.159	7	−1.8714
9	0.3(3)	0.072	14	−0.02(6)	−0.173	8	2.1939
10	0.2(3)	0.102	16	0.02(5)	−0.176	9	−1.2604
11	−0.3(3)	0.198	18	−0.12(5)	−0.174	10	1.9709
12	1.0(3)	0.171	20	−0.05(5)	−0.170	11	−0.9214
13	1.7(5)	0.257	22	0.22(5)	−0.164	12	1.3284
14	−0.1(16)	0.195	24	−0.04(5)	−0.157	13	−0.7074
15	−1.9(8)	0.287	26	−0.12(5)	−0.149	14	1.3832
16		0.198	28		−0.141	15	−0.5701
17	−0.8(5)	0.305	30		−0.134	16	1.2679
18	0.3(3)	0.190	32		−0.127	17	−0.4704
19	0.5(3)	0.316	34		−0.120	18	1.1474
20	−0.1(3)	0.175	36		−0.113	19	−0.3999
21	0.1(3)	0.323	38		−0.106	20	1.0459
22	0.8(3)	0.157	40		−0.100	21	−0.3451
23	−0.2(3)	0.330	42		−0.095	22	1.0018
24	−0.1(3)	0.136	44		−0.089	23	−0.3023
25	0.6(3)	0.337	46		−0.084	24	0.9333
26	0.6(3)	0.113	48		−0.079	25	−0.2681
27	−0.2(3)	0.345	50		−0.075	26	0.8724
28	−0.4(3)	0.088	52		−0.070	27	−0.2404
29	0.5(3)	0.355	54		−0.066	28	0.8957
30	−0.2(5)	0.061	56		−0.063	29	−0.2176
31		0.368	58		−0.059	30	0.7853
32		0.031	60		−0.056	31	−0.1963
33		0.383	62		−0.053	32	0.7919
34		−0.003	64		−0.050	33	−0.1798
35		0.405	66		−0.047	34	0.7633
36		−0.044	68		−0.045	35	−0.1651
37		0.435	70		−0.043	36	0.7444
38		−0.099				37	−0.1522
39		0.482				38	0.7164
40		−0.183				39	−0.1408
						40	0.6979

bands with the results found in AER (Atmospheric and Environmental Research [http://rtweb.aer.com]) line parameter database. This database includes all the line parameter information from HITRAN [7], including calculated values for line mixing coefficients from different bands of CO_2. These calculations were done by following the Energy Corrected Sudden approximation (ECS). A detailed description of the software used and the structure of the ECS format could be found in Ref. [19]. In Fig. 6a, the experimental values agree very well with the predicted values from EPG and ECS calculations for the $12201 \leftarrow 03301$ band. But $11101 \leftarrow 10002$ band shows comparatively higher observed values for line mixing coefficients than the calculated values as seen in Fig. 6b. The predicted trend for the line mixing values in $12201 \leftarrow 11102$ band is shown in Fig. 6c. And as can be noticed from the Fig. 6c, the e and f type transitions in this band show completely different trends from one another in terms of line mixing effects.

7. Conclusion

Spectral line parameters retrieved for the three Q branches ($12201 \leftarrow 03301$, $11101 \leftarrow 10002$ and $12201 \leftarrow 11102$) of CO_2 located near 15 μm region have been reported. A Voigt model could not produce best fit residuals for the transitions in these bands that are evident from the asymmetries observed in the fit residuals as seen in Fig. 2. To solve this problem, we constrained line positions and intensities, and fitted the spectra with a Voigt and line mixing profile. This choice significantly reduces the correlations between fitted parameters and improved the fits. Weak line mixing has been observed and measured in the fit of the $12201 \leftarrow 03301$ and $11101 \leftarrow 10002$ bands which yielded line mixing coefficients which reduced the fit residuals. Using Exponential Power Gap approximation (EPG) line mixing coefficients have been calculated taking all the input parameters (line position, intensity, broadening and lower state energy values) from HITRAN2012 database.

We have shown in Fig. 5a–c, with the exception of the e component of the $12201 \leftarrow 11102$ band, the calculated broadening coefficients agree well with the experimentally observed values for the three bands analyzed in this work. One interesting trend that could be noticed for the $12201 \leftarrow 11102$ band is the two distinguishable sets of values obtained for the e and f type transitions as shown in Fig. 5c. From the comparisons between measured and calculated values of line mixing coefficients (Fig. 6a and b) we conclude that line mixing effect is significant in the $12201 \leftarrow 03301$ and $11101 \leftarrow 10002$ bands of CO_2 and should be taken into account for obtaining a good fit. The figures show that the experimentally measured line mixing coefficients agree well with the calculated values. In Fig. 6c the EPG predicts two different trends for the e and f type transitions for line mixing parameters for the $12201 \leftarrow 11102$ band. From this study we infer that EPG calculations can predict well the line mixing effects.

Acknowledgements

The data recording for this study was done at the Canadian Light Source supported by NSERC, NRC, CIHR and the University of Saskatchewan. The work done at the University of Lethbridge is supported by funds from the Natural Sciences and Engineering Research Council of Canada and the NSERC CREATE AMETHYST program. The research performed at the College of William and Mary was supported by Grants from the National Aeronautics and Space Administration. The authors sincerely thank Dr. D. Chris Benner at the College of William and Mary for providing his multi-spectrum fitting software used in this study.

References

[1] H. Bovensmann, M. Buchwitz, J.P. Burrows, M. Reuter, T. Krings, K. Gerilowski, O. Schneising, J. Heymann, A. Tretner, J. Erzinger, Atmos. Meas. Tech. 3 (2010) 781–811.
[2] S. Franck, A. Block, W.V. Bloh, C. Bounama, H.-J. Schellnhuber, Y. Svirezhev, Planet. Space Sci. 48 (2000) 1099–1105.
[3] L.L. Strow, B.M. Gentry, J. Chem. Phys. 84 (1986) 1149–1156.
[4] B. Gentry, L.L. Strow, J. Chem. Phys. 86 (1987) 5722–5730.
[5] M.V. Tonkov, J. Boissoles, R. Le Doucen, B. Khalil, F. Thibault, J. Quant. Spectrosc. Radiat. Transfer 55 (1996) 321–334.
[6] A. Predoi-Cross, A.D. May, A. Vitcu, J.R. Drummond, J.-M. Hartmann, C. Boulet, J. Chem. Phys. 120 (22) (2004) 10520–10529.
[7] L.S. Rothman, I.E. Gordon, Y. Babikov, A. Barbe, D. Chris Benner, P.F. Bernath, M. Birk, L. Bizzocchi, V. Boudon, L.R. Brown, A. Campargue, K. Chance, E.A. Cohen, L.H. Coudert, V.M. Devi, B.J. Drouin, A. Fayt, J.-M. Flaud, R.R. Gamache, J.J. Harrison, J.-M. Hartmann, C. Hill, J.T. Hodges, D. Jacquemart, A. Jolly, J. Lamouroux, R.J. Le Roy, G. Li, D.A. Long, O.M. Lyulin, C.J. Mackie, S.T. Massie, S. Mikhailenko, H.S.P. Müller, O.V. Naumenko, A.V. Nikitin, J. Orphal, V. Perevalov, A. Perrin, E.R. Polovtseva, C. Richard, M.A.H. Smith, E. Starikova, K. Sung, S. Tashkun, J. Tennyson, G.C. Toon, Vl.G. Tyuterev, G. Wagner, J. Quant. Spectrosc. Radiat. Transfer 130 (2013) 4–50.
[8] D.C. Benner, C.P. Rinsland, V.M. Devi, M.A.H. Smith, D. Atkins, J. Quant. Spectrosc. Radiat. Transfer 53 (1995) 705–721.
[9] L.R. Brown, D.C. Benner, V.M. Devi, M.A.H. Smith, R.A. Toth, J. Mol. Struct. 742 (1–3) (2005) 111–122.
[10] K. Levenberg, Quart. Appl. Math. 2 (2) (1944) 164–168.
[11] D.W. Marquardt, J. Sot. Indust. Appl. Math. 11 (2) (1963) 431–441.
[12] V.M. Devi, D.C. Benner, L.R. Brown, C.E. Miller, R.A. Toth, J. Mol. Spectrosc. 242 (2007) 90–117.
[13] B.J. Drouin, D.C. Benner, L.R. Brown, M.J. Cich, T.J. Crawford, V.M. Devi, A. Guillaume, J.T. Hodges, E.J. Mlawer, D.J. Robichaud, F. Oyafuso, V.H. Payne, K. Sung, E.H. Wishnow, S. Yu, J. Quant. Spectrosc. Radiat. Transfer 186 (2017) 118–138.
[14] P. Sebald, C. Stein, R. Oswald, P. Botschwina, J. Phys. Chem. A 2013 (117) (2013) 13806–13814.
[15] E.T. Whittaker, G. Robinson, "The Calculus of Observations", Chapter 9, Blackie, Glasgow, 1926.
[16] N. Jacquinet-Husson, R. Armante, N.A. Scott, A. Chédin, L. Crépeau, C. Boutammine, A. Bouhdaoui, C. Crevoisier, V. Capelle, C. Boonne, N. Poulet-Crovisie, A. Barbe, D. Chris Benner, V. Boudon, L.R. Brown, J. Buldyreva, A. Campargue, L.H. Coudert, V.M. Devi, M.J. Down, B.J. Drouin, A. Fayt, C. Fittschen, J.-M. Flaud, R.R. Gamache, J.J. Harrison, C. Hill, Ø. Hodnebrog, S.-M. Hu, D. Jacquemart, A. Jolly, E. Jiménez, N.N. Lavrentieva, A.-W. Liu, L. Lodi, O.M. Lyulin, S.T. Massie, S. Mikhailenko, H.S.P. Müller, O.V. Naumenko, A. Nikitin, C. J. Nielsen, J. Orphal, V.I. Perevalov, A. Perrin, E. Polovtseva, A. Predoi-Cross, M. Rotger, A.A. Ruth, S.S. Yu, K. Sung, S.A. Tashkun, J. Tennyson, Vl.G. Tyuterev, J. Vander Auwera, B.A. Voronin, A. Maki, J. Mol. Spectrosc. 327 (2016) 31–72.
[17] A. Levy, N. Lacome, C. Chackerian Jr., K.N. Rao, A. Weber (Eds.), Academic Press, New York, 1992, pp. 261–337.
[18] A. Predoi-Cross, A.V. Unni, W. Liu, I. Schofield, C. Holladay, A.R.W. McKellar, D. Hurtmans, J. Mol. Spectrosc. 245 (2007) 34–51.
[19] F. Niro, K. Jucks, J.-M. Hartmann, J. Quant. Spectrosc. Radiat. Transfer 95 (2005) 469–481.
[20] R.R. Gamache, J. Lamouroux, J. Quant. Spectrosc. Radiat. Transfer 130 (2013) 158–171.
[21] S.A. Tashkun, V.I. Perevalov, R.R. Gamache, J. Lamouroux, J. Quant. Spectrosc. Radiat. Transfer 152 (2015) 45–73.
[22] R.R. Gamache, J. Lamouroux, V. Blot-Lafon, E. Lopes, J. Quant. Spectrosc. Radiat. Transfer 135 (2014) 30–43.